Abstract—Somatic growth parameters are used in age-structured stock assessment models, such as those used to assess the federally managed northern anchovy (*Engraulis mordax*); therefore, incorrect estimation of growth can cause errors that affect estimates from stock assessments. To our knowledge, we completed the first comprehensive investigation to model somatic and otolith growth of the central subpopulation of northern anchovy (CSNA), which has a range from Northern California to Baja California, Mexico, by using fishery-dependent and fishery-independent data. Five growth models were fitted to length-at-age data, including 2 models that account for seasonal growth oscillations, to determine the model that best described growth. Seasonal growth oscillations were found for the CSNA, and the best fitting models were the ones that accounted for seasonality. The fastest growth occurred during summer, and growth decreased 90% in winter. Large variations in length at age and extensive overlap of lengths across ages were found for the CSNA, typical observations for fish with an opportunistic life history strategy that respond rapidly to changing environmental conditions in dynamic ecosystems. Traditional growth models overestimated mean asymptotic length and underestimated the growth coefficient in comparison to results from the seasonal growth models. Accurately describing growth of the CSNA by accounting for seasonality is important to limiting biases that may propagate in stock assessments and management decisions.

Modeling somatic and otolith growth of the central subpopulation of northern anchovy (*Engraulis mordax*) by incorporating seasonality

Brittany D. Schwartzkopf (contact author)[1]
Emmanis Dorval[1,2]
Dianna L. Porzio[3]

Jonathan M. Walker[1,4]
Kelsey C. James[1]
Brad E. Erisman[1]

Email address for contact author: brittany.schwartzkopf@noaa.gov

[1] Fisheries Resources Division
Southwest Fisheries Science Center
National Marine Fisheries Service, NOAA
8901 La Jolla Shores Drive
La Jolla, California 92037

[2] Lynker
(under contract with NOAA Southwest
Fisheries Science Center)
202 Church Street SE #536
Leesburg, Virginia 20175

[3] Marine Region
California Department of Fish and Wildlife
2451 Signal Street, AltaSea Berth 59
San Pedro, California 90731

[4] Cooperative Institute for Marine, Earth, and
Atmospheric Systems
University of California Santa Cruz
1156 High Street
Santa Cruz, California 95064

Somatic growth rate is an important determinant of population growth and recruitment in marine fish species (Kerns and Lombardi-Carlson, 2017). Clupeoids have an opportunistic life history strategy, which is characterized by rapid somatic growth, high mortality rates, short life spans, and protracted spawning seasons in response to environmental conditions (Blaxter and Hunter, 1982; Armstrong and Shelton, 1990; Winemiller and Rose, 1992). Clupeoids opportunistically utilize favorable environmental conditions that vary on different scales, such as the conditions of the California Current Ecosystem (CCE), which vary on daily, interannual, and decadal scales (McClatchie, 2014), leading to high variation in growth rates of individuals and large annual and seasonal fluctuations in growth (Spratt, 1975; Mallicoate and Parrish, 1981; Cubillos et al., 2001). The rapid response of fish to favorable environmental conditions leads to changes in growth rate and

mortality that contribute to natural, large fluctuations in recruitment and population sizes of clupeoids (Blaxter and Hunter, 1982; Thayer et al., 2017; Sydeman et al., 2020).

Estimating somatic growth rate correctly is important, as it is a primary biological characteristic used in fisheries assessments, management, and research (Kerns and Lombardi-Carlson, 2017). Somatic growth characteristics are used as parameters in age-structured stock assessment models, such as those used to assess biomass of coastal pelagic species (CPS) in the North Pacific Ocean along the West Coast of the United States (Methot, 1989; Crone et al., 2019; Kuriyama et al., 2020, 2022). Incorrectly estimating growth characteristics, whether as a result of aging errors or use of improper growth models, can cause errors that affect estimates of other biological characteristics, such as age at maturity, length at age, and weight at age, and estimates of

fishery indices, such as catch at age and biomass, that depend on age data (Reeves, 2003). Incorrect estimation of growth characteristics can also lead to errors in estimates of recruitment and total allowable catch allocated to fisheries in assessment models (Reeves, 2003) and to errors that can significantly mask relationships between stocks and recruitment and between environmental factors and year-class strength (Fournier and Archibald, 1982; Richards et al., 1992).

Many fishes have seasonal oscillations in growth, and not incorporating this seasonality in data analysis when it is present can lead to incorrect estimation of somatic growth characteristics (Liu et al., 2021). Misspecifications of growth models can affect the computation of recruitment (age-0 fish) and estimation of biomass (age-1+ fish), information that is used to manage CPS stocks and set harvest guidelines (Reeves, 2003; Stawitz et al., 2019; Kuriyama et al., 2020). Unless seasonal effects can be explicitly accounted for in growth models, only information for samples collected from the same season should be compared (Shoup and Michaletz, 2017), an important consideration when samples are collected year-round. When seasonality was ignored for small species of commercial importance in coastal areas of the China Seas, the fat greenling (*Hexagrammos otakii*) and yellow croaker (*Larmichthys polyactis*), Liu et al. (2021) found that biological reference points were underestimated, an outcome that was attributed to incorrect estimation of growth parameters resulting from ignoring seasonal growth patterns. The underestimation of biological reference points indicates that a species is less productive than it actually is and can result in the loss of potential yield (Liu et al., 2021).

The most commonly used function to model fish growth is the von Bertalanffy growth function (VBGF) (von Bertalanffy, 1938; Ogle et al., 2017), which does not account for seasonality. Several models that modify the VBGF have been proposed to account for seasonal growth oscillations (Ogle et al., 2017). Seasonal growth models, like the 2 commonly used functions of Somers (1988) and Pauly et al. (1992), account for periods of faster and slower growth within a year. The Somers (1988) function allows modeled growth to be reduced, completely stopped, or decreased, whereas the function of Pauly et al. (1992) does not allow decreasing growth but can be used to model prolonged periods of no growth.

The northern anchovy (*Engraulis mordax*) is one of the most abundant forage fish species in the CCE and is consumed by many different species (e.g., marine mammals, seabirds, salmon, tunas, and sharks), making it an important part of the food web (Koehn et al., 2017; Thompson et al., 2022). Similar to other clupeoid species, the northern anchovy is characterized by high interannual variability in recruitment success and population abundance in response to environmental conditions (Methot, 1983; MacCall et al., 2016; Thayer et al., 2017; Sydeman et al., 2020). Additionally, the northern anchovy is a multiple batch spawner with a protracted spawning season; spawning may occur year-round, but peak spawning generally occurs from January through April (Hunter and Macewicz, 1980; Hunter and Leong, 1981; Dorval et al., 2018).

Three subpopulations, the northern, central, and southern subpopulations, are recognized for northern anchovy on the basis of morphometric and meristic characteristics (McHugh, 1951; Vrooman et al., 1981); however, Lecomte et al. (2004) did not detect genetic structure across its range. The central subpopulation of northern anchovy (CSNA) ranges between San Francisco, California, and the middle of the Baja California Peninsula in Mexico. The CSNA is managed in U.S. waters under the Coastal Pelagic Species Management Plan (PFMC, 2019) and was last assessed in 2021 (Kuriyama et al., 2022), 26 years after the previous assessment. The current assumption is that the overall population size is at or around its highest level since the development of quantitative monitoring in the CCE around 70 years ago (Thompson et al., 2019, 2022).

No recent work has included examination of somatic growth of the CSNA, despite its ecological role in the CCE and the importance of growth estimates in informing stock assessments. The most recent work examining growth of northern anchovy through the adult stage was done by Parrish et al. (1985), and a few limited studies have provided values of growth parameters (i.e., mean asymptotic length [L_∞] and the growth coefficient [K]) calculated by using traditional growth models (Spratt, 1975; Cisneros et al., 1990). In no work have seasonal growth oscillations of northern anchovy been modeled by using traditional growth models (e.g., the VBGF) with data on fish collected year-round, but seasonal variations in growth of northern anchovy have been generally observed (Mallicoate and Parrish, 1981; Methot, 1983; Parrish et al., 1985; Butler, 1989; Takahashi et al., 2012). Seasonal growth oscillations have been reported for other engraulids (Palomares et al., 1987; Cubillos and Arancibia, 1993; Bellido et al., 2000; Bilgin et al., 2013; Cerna and Plaza, 2016). Northern anchovy reportedly live up to 8 years (Mallicoate and Parrish, 1981), but older individuals (i.e., age-4+ fish) are thought to be relatively scarce (Collins, 1969; Spratt, 1975; Mallicoate and Parrish, 1981; Parrish et al., 1985). Understanding the age structure and growth patterns of northern anchovy is important, as it is a model species for examining and projecting the effects of climate change on clupeoids and marine communities in the CCE and on fisheries management (Muhling et al., 2019, 2020; Tommasi et al., 2021).

The goal of this study was to update the age and growth patterns of the CSNA to inform future stock assessments. The objectives were to model growth and determine whether the CSNA has seasonal growth oscillations 1) by comparing estimates from 3 growth models, the Gompertz, logistic, and von Bertalanffy growth functions, to integer age data; 2) by calculating fractional ages and comparing estimates between the VBGF and 2 models allowing seasonal growth oscillations (Somers, 1988; Pauly et al., 1992); and 3) by examining seasonal variations in the relationships of weight to body length and of body length to otolith length.

Materials and methods

Data sources and collection methods

Samples from the CSNA were collected during both fishery-dependent and fishery-independent surveys from 2015 through 2021. Fishery-independent data were collected as part of acoustic-trawl surveys of CPS conducted aboard the NOAA Ships *Reuben Lasker* and *Bell M. Shimada* by the NOAA Southwest Fisheries Science Center (SWFSC) in summer and fall (June–September) for each year in 2015–2021, as well as in spring (March and April) in 2017 and 2021 (Dorval et al., 2018; Stierhoff et al., 2019; Zwolinski et al., 2019; Stierhoff et al., 2020, 2021a, 2021b). The primary objectives of the SWFSC trawl survey are 1) to survey the distributions and abundances of CPS and their abiotic environments in the CCE and 2) to measure size–frequency distributions and to gather life history information (Stierhoff et al., 2020; Renfree et al., 2022), in order to produce length and age composition data for use in acoustic biomass estimation and stock assessment models.

Sagittal otolith samples were collected by using a 2-stage sampling design that follows best practices (Miranda and Colvin, 2017). For the first stage, a maximum of 75 individuals of the CSNA were randomly collected from each nighttime trawl haul, and each individual fish was measured for standard length (SL) to the nearest millimeter and for total weight (TW) to the nearest 0.5 g. For the second stage, 25 individuals that had lengths that encompassed the size distribution of the first-stage samples were selected for otolith extraction and aging by the SWFSC. A complete description of the data collection methods of the SWFSC trawl survey can be found in Dorval et al. (2022) and Schwartzkopf et al. (2022).

Fishery-dependent samples were collected by the California Department of Fish and Wildlife (CDFW) during port sampling of commercial fishery landings. The CDFW sampling plan for CPS is based on a stratified-random design, where samples are collected during 12 random days within each month of the year for each of the port areas where the majority of landings occur: the areas of Monterey, Santa Barbara, and Los Angeles. The majority of fish were collected off Monterey, but in 2016 some additional samples were collected off Los Angeles. For each vessel from which landings were sampled, 25 fish were randomly selected throughout the offload period and brought back to a lab, where they were measured for SL to the nearest millimeter and for TW to the nearest 0.1 g. Otoliths were then extracted for aging to be completed by the CDFW. A complete description of the design and methods of data collection by the CDFW can be found in Dorval et al. (2022). The combined data from fishery-dependent and fishery-independent surveys used in the CSNA stock assessment models were collected year-round, allowing seasonality to be explored.

Age determination

Whole (i.e., not sectioned) otoliths were immersed in distilled water in a glass dish with a black background for no longer than 3 min, counts were made of the number of annuli observed on the distal side of the otolith, and edge type was determined. Aging was conducted by using a dissecting microscope with reflected light at a magnification of 25×. An annulus is defined as the interface between an inner translucent growth increment and the successive outer opaque growth increment (Collins and Spratt, 1969; Yaremko, 1996; Schwartzkopf et al., 2022). To our knowledge, annual age determination has not been validated for the northern anchovy, but first annulus formation and annual age determination has been validated for the European anchovy (*E. encrasicolus*) (Aldanondo et al., 2016; Uriarte et al., 2016; Basilone et al., 2020); therefore, we assumed this validation held true for the northern anchovy.

Integer age was assigned on the basis of a June birthdate by using the capture date and interpretation of the most distal pair of increments (Collins and Spratt, 1969; Schwartzkopf et al., 2022). Because samples were collected year-round, fractional age was also determined by dividing the integer age by 12 and by using a June birthdate. Age data from both fishery-independent and fishery-dependent surveys and from all years were combined because we were interested in modeling growth of the CSNA as a whole (similar to the modeling done in the stock assessment) and because effects of these factors (i.e., year and type of survey) are beyond the scope of this work. Sample sizes by age for each month of sampling can be found in Supplementary Table 1.

Relationships of standard length to weight and to otolith length

We fit a generalized linear model (GLM) incorporating *season* for all individuals measured for length and weight (sample size [n]=19,209) to examine the weight–length relationship of the CSNA, similar to the work done by Palance et al. (2019). The GLM was fitted by using the base function glm in R (vers. 4.2.1; R Core Team, 2022) and has the following structure:

$$l\left(\widehat{TW}_{i,j}\right) = \beta_0 + \beta_1 Season_j + \beta_2 \log_e\left(SL_{i,j}\right), \quad (1)$$

where l = the log link function;

$\widehat{TW}_{i,j}$ = the total weight (in grams) of fish i in season j;

$Season$ = a categorical factor with fall, winter, spring, and summer; and

$SL_{i,j}$ = the standard length (in millimeters) of fish i in season j.

Note that $\widehat{TW}_{i,j}$ has a gamma distribution, with the mean calculated as follows:

$$\widehat{TW}_{i,j} = e^{\left(\beta_0 + \beta_1 Season_j + \beta_2 \log_e\left(SL_{i,j}\right)\right)}. \quad (2)$$

The variance of the gamma distribution was calculated as follows:

$$\frac{\widehat{TW}_{i,j}^{\,2}}{\nu}, \quad (3)$$

where ν = a dispersion parameter estimated during fitting.

The season was determined on the basis of the month of capture, with months of capture from September through November assigned to the fall season, the months from December through February considered to be winter, the months from March through May assigned to spring, and the months from June through August considered to be summer. The model fit was determined with the adjusted amount of deviance accounted for by a GLM, D^2 (Guisan and Zimmermann, 2000), calculated by using the Dsquared function in the R package modEvA, vers. 3.8.4 (Barbosa et al., 2013). The effect of season among all season pairs was compared by running the GLM 4 times, each time with a different season as the intercept, and evaluating the *t*-statistic for every season effect (e.g., if fall was the intercept, the *t*-statistics for the individual effects of winter, spring, and summer were evaluated relative to the fall intercept).

We chose a random subset of otoliths (n=2036), from fish collected during both SWFSC trawl surveys and CDFW port sampling that had lengths that encompassed the size distribution within each season, to examine the relationship of SL to otolith length and to confirm that otolith growth reflects somatic growth. The right-side otolith was chosen when possible and was imaged by using a dissecting microscope with an AmScope camera (United Scope LLC, Irvine, CA) and analyzed with the R package shapeR (vers. 0.1-5; Libungan and Pálsson, 2015) to calculate otolith length (Feret length) at the time of capture. We fitted a linear model that has *season* as a variable and has the following structure:

$$\left(SL_{i,j}\right) = \beta_0 + \beta_1 Season_j + \beta_2\left(OL_{i,j}\right)$$
$$+ \beta_3\left(Season_j OL_{i,j}\right), \tag{4}$$

where $OL_{i,j}$ = the otolith length (in millimeters) of fish i in season j.

A model with an interaction between *season* and $OL_{i,j}$ was chosen, given that previous work on CPS found reduced effects of seasonality on otolith length as the length of fish increased (Thomas, 1983). A model with no interaction term was also fitted, but the model with the interaction term had a lower Akaike information criterion (AIC) than the model with no interaction term (AIC: 13632 and 13800, respectively) and was deemed a better fit (Akaike, 1973; Burnham and Anderson, 2002; Burnham et al., 2011). The effect of season among all season pairs was compared by running the linear model 4 times, each time with a different season as the intercept, and evaluating the *t*-statistic for every season effect (e.g., if fall was the intercept, the *t*-statistics for the individual effects of winter, spring, and summer were evaluated relative to the fall intercept). Visual examination of the diagnostic plots of both of the models used to examine the relationships of weight to length and of length to otolith length revealed that the assumptions of normality and homogeneity of variance were met.

Somatic growth modeling

We fitted 5 growth models to length-at-age data to examine which model best describes somatic growth of the CSNA. The Gompertz growth model (Gompertz, 1825) is as follows (Ricker, 1975; Ogle et al., 2017):

$$L_t = L_\infty e^{-e^{-g^*\left(t-t^*\right)}}, \tag{5}$$

where L_t = the mean length at age t;
L_∞ = the mean asymptotic length (i.e., the maximum mean length for the population);
g^* = the instantaneous growth rate at the inflection point t^*; and
t^* = the maximum instantaneous growth rate.

The logistic growth model (Campana and Jones, 1992; Ogle et al., 2017) is as follows:

$$L_t = L_\infty\left[1 - e^{-g_{-\infty}\left(t-t^*\right)}\right], \tag{6}$$

where $g_{-\infty}$ = the positive instantaneous growth rate as age approaches negative infinity.

The final 3 models are parameterizations or modifications of the VBGF (von Bertalanffy, 1938), which has the following common foundation:

$$L_t = L_\infty\left(1 - e^{-q}\right), \tag{7}$$

where q = at least a function of t.

For the VBGF attributable to Beverton and Holt (1957), q takes this form:

$$q = K\left(t - t_0\right), \tag{8}$$

where K = the growth coefficient, a measure of the exponential rate at which L_t approaches L_∞; and
t_0 = the theoretical age at which L_t is zero.

As CPS have seasonal variations in their somatic growth rates, 2 modifications to the VBGF were fitted to model seasonal oscillations in growth, similar to the adjustments to the VBGF done by Ogle (2017). The first modification of the VBGF is from Hoenig and Choudaray Hanumara (1982) and Somers (1988), with a clarification by García-Berthou et al. (2012). In this model, hereafter referred to as the *Somers model*, q takes this form (Ogle, 2017):

$$q = K\left(t - t_0\right) + \frac{CK}{2\pi}\sin\left(2\pi\left(t - t_s\right)\right)$$
$$- \frac{CK}{2\pi}\sin\left(2\pi\left(t_0 - t_s\right)\right), \tag{9}$$

where t_s = the inflection point, or the amount of time between time zero and the start of the convex portion of the first sinusoidal growth oscillation; and
C = the proportional decrease in growth at the depth of the growth oscillation, normally the "winter" season.

If $C=0$ (i.e., if there is no seasonal oscillation in mean length), the equation reduces to the VBGF. If $C>0$ and $C<1$, the increase in mean length is reduced but does not stop; if $C=1$, the increase in mean length comes to a complete stop; and if $C>1$, mean length decreases during "winter." The time of the year when growth is slowest, known as the *winter point* (WP), was calculated as follows:

$$WP = t_s + 0.5. \tag{10}$$

Pauly et al. (1992) argued that a C greater than 1 is biologically improbable for fish vertebrates whose skeletons largely preclude shrinkage in length and, therefore, proposed a modification to the Somers model in which mean length was not allowed to decrease. In this model, hereafter referred to as the *Pauly model*, q takes this form:

$$q = K'\left(t' - t_0\right) + \frac{K'\left(1 - NGT\right)}{2\pi}\sin\left(\frac{2\pi}{1 - NGT}\left(t' - t_s\right)\right)$$
$$- \frac{K'\left(1 - NGT\right)}{2\pi}\sin\left(\frac{2\pi}{1 - NGT}\left(t_0 - t_s\right)\right), \tag{11}$$

where NGT = the *no growth time*, the length of the no growth period as a fraction of a year.

The age t' is found by "subtracting from the real age (t) the total no-growth time occurring up to age t" (Pauly et al., 1992; Ogle, 2017). Pauly et al. (1992) suggested using K' to minimize confusion with K in the VBGF as the units changed from year^{-1} to $(1-NGT)^{-1}$.

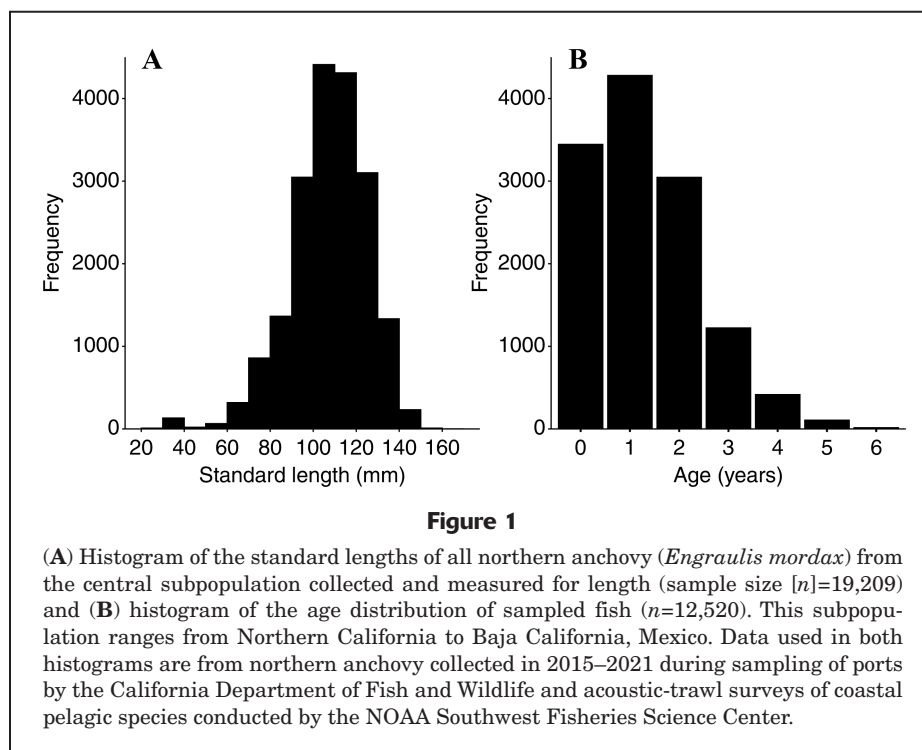Model parameters and 95% confidence intervals were estimated by using nonlinear least squares regression with the R package FSA (vers. 0.9.3; Ogle et al., 2022) and the nlsBoot function in the R package nlstools (vers. 2.0-0; Baty et al., 2015), respectively. Starting values were obtained by visually fitting the models to the observed data, and alternative starting values were used to confirm a global minimum was obtained. The best fitting model was chosen by using the AIC values (Akaike, 1973; Ogle, 2017), with the best fitting model having the lowest AIC and other models ranked according to the differences in their AIC values from that of the best model (Burnham and Anderson, 2002; Burnham et al., 2011).

Results

Length and age structure

A total of 19,209 individuals were measured for length and weight, and 12,520 otoliths from fish collected during both fishery-dependent and fishery-independent surveys were aged from 2015 to 2021 and used in subsequent analyses. Lengths from all measured fish ranged from 23 to 164 mm SL, lengths from aged fish ranged from 44 to 164 mm SL, and ages ranged from 0 to 6 years (Fig. 1, A and B). Age-0 and age-1 fish accounted for 62% of the samples, and a steady decline in the frequency of older aged fish was observed, with age-4+ fish accounting for 4% of the samples (Fig. 1B). All fish <69 mm SL were age 0.

The GLM used to examine the relationship of weight to length was significant ($P<0.0001$) and fit the data well ($D^2=0.95$). Winter did not differ from spring ($t=0.36$, $P=0.71$), but all other seasons were significantly different

Figure 1

(**A**) Histogram of the standard lengths of all northern anchovy (*Engraulis mordax*) from the central subpopulation collected and measured for length (sample size [n]=19,209) and (**B**) histogram of the age distribution of sampled fish (n=12,520). This subpopulation ranges from Northern California to Baja California, Mexico. Data used in both histograms are from northern anchovy collected in 2015–2021 during sampling of ports by the California Department of Fish and Wildlife and acoustic-trawl surveys of coastal pelagic species conducted by the NOAA Southwest Fisheries Science Center.

from each other ($P<0.0001$), including fall from winter ($t=4.11$), spring ($t=5.12$), and summer ($t=36.58$) and winter from summer ($t=22.57$) and spring ($t=-31.30$) (Table 1). Looking at the model predictions, fish from summer had a larger weight at a given length (Fig. 2A). Although fish from winter and spring statistically differed from fish from fall, the model predictions look similar among these 3 seasons (Fig. 2A). Full results from the GLM can be found in Supplementary Table 2.

A total of 2036 otoliths were imaged to calculate otolith length. The linear model of the relationship of SL to otolith length was significant ($P<0.05$) and fit the data well (coefficient of multiple determination [R^2]=0.90). Fall, winter, and spring did not differ from each other, including fall from winter ($t=1.43$, $P=0.15$) and spring ($t=-0.31$, $P=0.75$) and winter from spring ($t=-1.58$, $P=0.11$), but summer differed from all the other seasons (from fall: $t=9.74$; from winter: $t=8.99$; and from spring: $t=7.77$; $P<0.0001$) (Table 2). Looking at the model predictions, otolith length was greatest in winter, followed by fall, spring, and summer for small fish (less than ~120 mm SL) (Fig. 2B). As fish length increased, the effects of seasonality were reduced, and otolith length was similar between seasons for fish of the same size (Fig. 2B). Full results from the linear model can be found in Supplementary Table 3.

Somatic growth modeling

Large variation in length at age was found among individuals from the CSNA, with higher variation in length at age for young fish (<2 years) and smaller variation for old fish (>5 years) (Fig. 3, A and B). The von Bertalanffy, Gompertz, and logistic growth functions yielded asymptotic growth patterns when fitted to both integer and fractional age data (Fig. 3, A and B). Curves for modeled length at age are nearly identical for all 3 models at all ages (Fig. 3, A and B), with similar parameter estimates within each age data set (Table 3). Notably, parameter
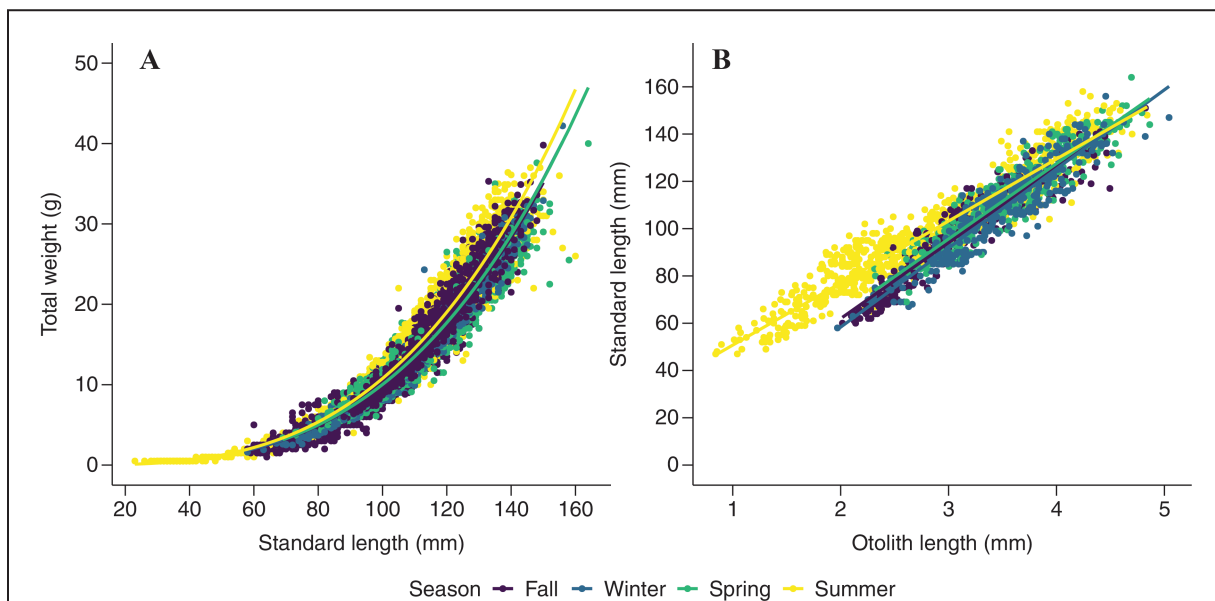

Table 1

Equations used to determine the relationship of total weight (TW) to standard length (SL) in the general linear model for each season for the central subpopulation of northern anchovy (*Engraulis mordax*). This subpopulation ranges from Northern California to Baja California, Mexico. Parameter estimates for each season are given within the equation. For example, the estimates from the fall model are as follows: −12.085 for the intercept and 3.122 for the slope. The model was fitted to a combination of fishery-independent and fishery-dependent data from 2015 through 2021, and the sample size (n) for each season is provided.

Season	n	Model equation
Fall	5788	$TW = e(-12.085)SL^{3.122}$
Winter	5743	$TW = e(-12.071)SL^{3.122}$
Spring	5603	$TW = e(-12.073)SL^{3.122}$
Summer	2075	$TW = e(-12.001)SL^{3.122}$

Figure 2

Relationships (**A**) between total weight and standard length and (**B**) between standard length and otolith length by season for the central subpopulation of northern anchovy (*Engraulis mordax*) that ranges from Northern California to Baja California, Mexico. The lines represent the predictions from the growth models used in this study, and the points represent the raw data for fish collected during fishery-independent and fishery-dependent surveys from 2015 through 2021.

Table 2

Equations used to determine the relationship of standard length (SL) to otolith length (OL) in the linear model for each season for the central subpopulation of northern anchovy (*Engraulis mordax*). This subpopulation ranges from Northern California to Baja California, Mexico. Parameter estimates for each season are given within the equation. For example, the estimates from the fall model are as follows: −2.316 for the intercept and 32.134 for the slope. The model was fitted to a combination of fishery-independent and fishery-dependent data from 2015 through 2021, and the sample size (*n*) for each season is provided.

Season	*n*	Model equation
Fall	511	$SL = -2.316 + 32.134(OL)$
Winter	317	$SL = -8.584 + 33.460(OL)$
Spring	354	$SL = 0.042 + 31.864(OL)$
Summer	854	$SL = 24.491 + 26.243(OL)$

estimates differed between the integer age and fractional age data sets for the same model, with estimates of L_∞ being greater and estimates of the growth coefficients (i.e., K, g^*, $g_{-\infty}$) being lower with a given model fitted to the integer age data set than with that model fitted to the fractional age data set (Table 3). For

example, with the VBGF, L_∞ was estimated at 130.6 mm SL and K was estimated at 0.52 year^{-1} when the integer age data set was used, whereas L_∞ was estimated at 125.1 mm SL and K was estimated at 0.72 year^{-1} when the fractional age data set was used. The VBGF was the best fitting model for both the integer age and fractional age data sets, followed by the Gompertz and logistic models (Table 4).

When modeling seasonal oscillations of growth, the Somers model and Pauly model were indistinguishable (Fig. 4, Table 5) and fit the data better than the VBGF, although the Somers model had the lowest AIC value and was deemed the best fit. With the Somers model, L_∞ was estimated at 126.2 mm SL and K was estimated at 0.68 year^{-1}. Growth was fastest during the first year of growth. There was evidence of a 90% reduction in growth during the winter season ($C=0.9$), and the month of slowest estimated growth was December (WP=0.62). We fit a VBGF to integer age data from August and September to compare parameter outputs when seasonality was removed. Data from August and September were chosen because data for these months included information for individuals with the full range of ages in sufficient numbers (Suppl. Table 1). When seasonality was removed from this model fitted with integer age data, L_∞ was estimated at 126.9 mm SL and K was estimated at 0.78 year^{-1}, values similar to the parameter estimates from the Somers model.
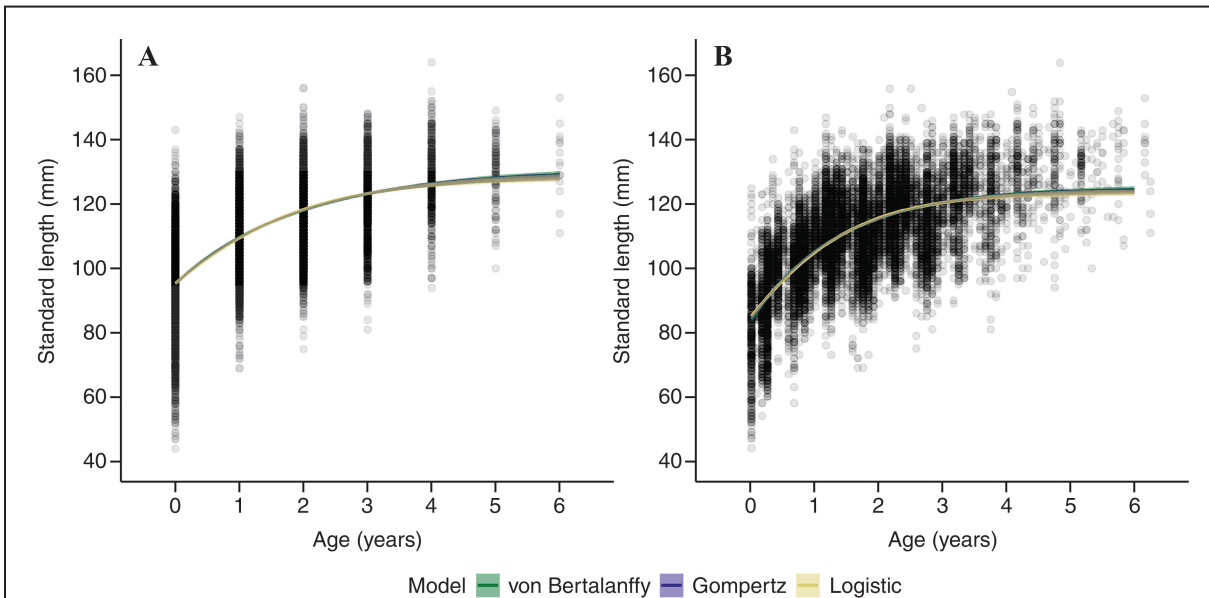

Figure 3

Growth curves from von Bertalanffy, Gompertz, and logistic growth functions fitted to (**A**) length-at-integer-age data and (**B**) length-at-fractional-age data for the central subpopulation of northern anchovy (*Engraulis mordax*) that ranges from Northern California to Baja California, Mexico. The solid lines indicate model predictions based on observed data, and the shaded areas indicate the 95% confidence intervals for these predictions. The black circles (with transparency) indicate the raw data points for individuals. The data used in the models are for fish collected from 2015 through 2021 during fishery-independent and fishery-dependent surveys. Parameter estimates from the model fits are provided in Table 3.

Table 3

Equations used in 3 growth models to estimate the mean length at age t (L_t) for the central subpopulation of northern anchovy (*Engraulis mordax*) that ranges from Northern California to Baja California, Mexico. Parameter estimates from each model are given within the equation; for example, estimates from the first equation for the von Bertalanffy growth function are as follows: 130.6 mm in standard length for the mean asymptotic length, 0.52 year^{-1} for the growth coefficient, and 2.51 years for the theoretical age at which L_t is zero. The von Bertalanffy, Gompertz, and logistic growth functions were fitted to both integer and fractional age data for fish collected from 2015 through 2021 during fishery-independent and fishery-dependent surveys.

Data set	Model	df	Model equation
Integer ages	von Bertalanffy	12,517	$L_t = 130.6\left[1 - e^{-0.52(t+2.51)}\right]$
	Gompertz	12,517	$L_t = 129.5e^{\left(-\left(\frac{1}{0.60}\right)e^{-0.60(t+1.95)}\right)}$
	Logistic	12,517	$L_t = 128.6\left[1 + e^{-0.68(t+1.52)}\right]^{-1}$
Fractional ages	von Bertalanffy	12,517	$L_t = 125.1\left[1 - e^{-0.72(t+1.53)}\right]$
	Gompertz	12,517	$L_t = 124.3e^{\left(-\left(\frac{1}{0.83}\right)e^{-0.83(t+1.14)}\right)}$
	Logistic	12,517	$L_t = 123.7\left[1 + e^{-0.93(t+0.84)}\right]^{-1}$

Table 4

Statistical measures of fit for von Bertalanffy, Gompertz, and logistic growth functions fitted to data sets of lengths at integer and fractional ages for northern anchovy (*Engraulis mordax*) of the central subpopulation collected during 2015–2021. This subpopulation ranges from Northern California to Baja California, Mexico. For each model, number of parameters (K), the Akaike information criterion (AIC) and the difference in its AIC value from that of the best model (the one with the lowest AIC) (ΔAIC) are provided.
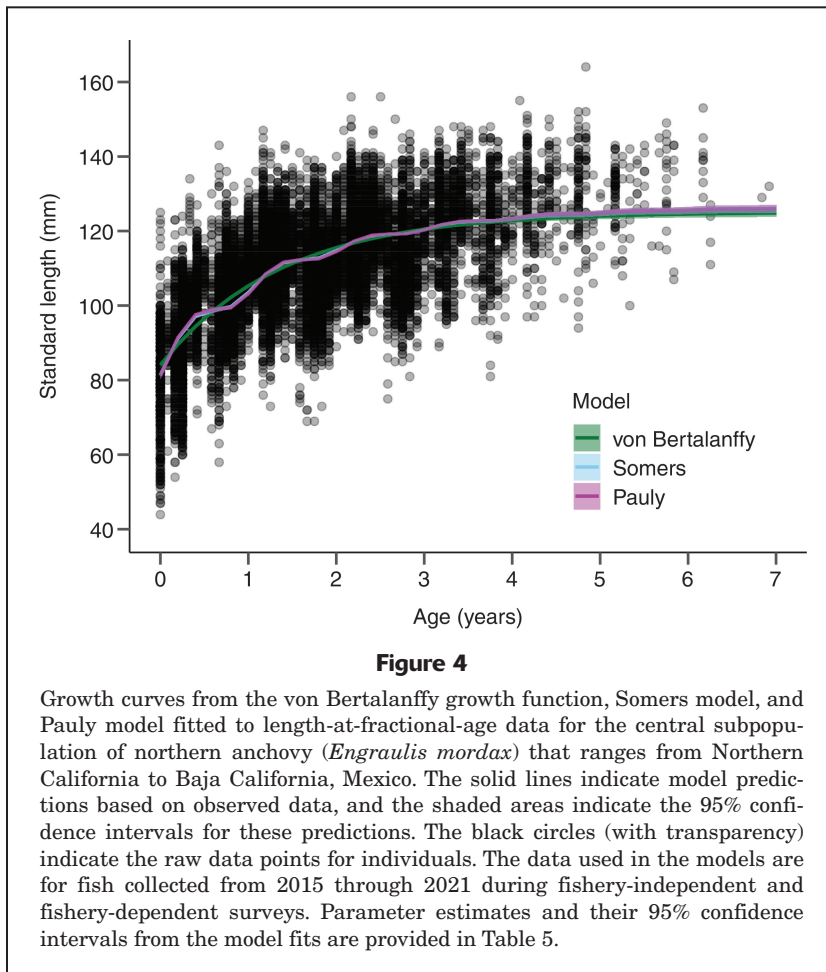
Data set	Model	K	AIC	ΔAIC
Integer ages	von Bertalanffy	4	97,208.86	0.00
	Gompertz	4	97,221.82	12.95
	Logistic	4	97,235.67	26.81
Fractional ages	von Bertalanffy	4	96,428.34	0.00
	Gompertz	4	96,477.62	49.28
	Logistic	4	96,526.79	98.45

Discussion

The results of this study provide an update of the understanding of CSNA growth patterns, given that the last work examining growth of the CSNA through the adult stage was completed 38 years ago (i.e., Parrish et al., 1985). We found patterns in somatic growth of the CSNA that are typical of *r*-selected and opportunistic species, which have small body sizes, low maximum ages, and high growth rates (Adams, 1980; Winemiller and Rose, 1992; King and McFarlane, 2003). Additionally, fast growth during the first year of life, high individual variation in growth rates, and seasonal fluctuations in growth, as found in our study, are characteristic of CPS in upwelling environments (Cubillos et al., 2001; Takahashi et al., 2012). High variability in growth rates among individuals from the CSNA has been postulated to lead to increased population growth rates due to size-dependent mortality and, therefore, to lead to increased population size (Lo et al., 1995). The growth characteristics of the CSNA contribute to high interannual variability in recruitment success and population abundance observed for this population of northern anchovy (Lasker, 1981; MacCall et al., 2016; Thayer et al., 2017).

Large variations in length within each age class, extensive overlap of lengths across ages, rapid somatic growth during the first year of life, and high proportions of young fish (<4 years old) with scarcity of older individuals have been found in studies investigating the CSNA (Collins and Spratt, 1969; Spratt, 1975; Mais, 1981; Mallicoate and Parrish, 1981; Parrish et al., 1985) and other species of *Engraulis* (Bacha et al., 2010; Cerna and Plaza, 2016). Spratt (1975) modeled growth of individuals from the CSNA collected during both fishery-dependent and fishery-independent surveys and found a higher L_∞ (165 mm SL) and lower K (0.29 year^{-1}) than the estimates for those parameters from our study, and Cisneros et al. (1990) found an L_∞ of 153 mm SL and a K of 0.7 year^{-1} for northern anchovy collected from the Gulf of California in Mexico (the southern subpopulation). The higher L_∞ and

Figure 4

Growth curves from the von Bertalanffy growth function, Somers model, and Pauly model fitted to length-at-fractional-age data for the central subpopulation of northern anchovy (*Engraulis mordax*) that ranges from Northern California to Baja California, Mexico. The solid lines indicate model predictions based on observed data, and the shaded areas indicate the 95% confidence intervals for these predictions. The black circles (with transparency) indicate the raw data points for individuals. The data used in the models are for fish collected from 2015 through 2021 during fishery-independent and fishery-dependent surveys. Parameter estimates and their 95% confidence intervals from the model fits are provided in Table 5.

temperatures and the increase in productivity from upwelled, nutrient-rich waters that stimulates growth of phytoplankton (Checkley and Barth, 2009; Jacox et al., 2018). Although productivity is increased during summer months, food aggregations are patchy and may be composed of prey of different levels of quality (Lasker and Zweifel, 1978; Litz et al., 2010), potentially resulting in large, opportunistic feeding events of variable nutritional quality for some individuals of the CSNA. Differences in the quality of prey encountered between individuals from the CSNA can contribute to high variability in their growth rates.

Additionally, the protracted spawning season of the CSNA may also contribute to large variations of length within each age class, especially at younger ages (Methot, 1983). For example, an age-0 fish born early in the year would be larger in length than an age-0 fish born later in the year when collected at the same time. The use of fractional ages in our work helped to address this phenomenon, but the birthdates of individual fish are still unknown. The lack of birthdates may bias any estimate of actual somatic growth; therefore, caution should be taken when making interpretations.

Somatic growth of the CSNA was slowest in winter, a result that is linked to cool sea-surface temperatures and reproductive strategies (Cubillos and Arancibia, 1993; Cubillos et al., 2002; Bilgin et al., 2013). The peak CSNA spawning season is from January through April (Hunter and Leong, 1981; Reiss et al., 2008); therefore, the slowest growth in December aligns with a shift from somatic growth to gametic growth in preparation for spawning. The duration of spawning season increases with female length, weight, and age, and although a large majority of individuals are mature by age 0, older females contribute disproportionately more to total annual egg production than first-time spawners (Hunter and Macewicz, 1985; Parrish et al., 1986; Schwartzkopf et al., 2022). The reduction in seasonality in somatic growth of older individuals is likely due to the increased investment in reproduction over more of the year and reduced somatic growth at older ages (>3 years) (Armstrong and Shelton, 1990; Kozlowski, 1996). If fish mature at different ages, individual variability in reproductive investment may also contribute to high variability in growth rates among individuals (Brosset et al., 2016; Claireaux et al., 2021).

Large variations and extensive overlaps in length at age present challenges in estimating other life history characteristics and consequently in conducting stock

lower *K* found by Spratt (1975) reflect their sample distribution, with lengths of sampled fish ranging from 88 to 160 mm SL and no age-0 fish. Without large and old fish, L_∞ is underestimated and *K* is overestimated (Bolser et al., 2018); therefore, it follows that the absence of small and young fish would result in overestimation of L_∞ and underestimation of *K*, as is revealed when comparing estimates from Spratt (1975) and those from our study. Cisneros et al. (1990) collected fish with size and age ranges similar to the fish collected for our study (~50–140 mm SL, 0–5 years), likely contributing to similar *K* values. However, they modeled growth using length–frequency analysis instead of ages calculated from otolith readings, possibly driving the differences in L_∞.

Seasonal CSNA growth oscillations and large variations of length within each age class were not unexpected and reflect the life history characteristics of this species in response to environmental conditions of the CCE. Somatic growth of the CSNA was most rapid during the summer months in our study, with increased length at a given weight in summer compared to that in other seasons, a result that also has been found for northern anchovy collected in the CCE (Palance et al., 2019). This rapid summer growth is likely in response to warmer sea-surface

Table 5

Estimates and 95% confidence intervals for parameters of the von Bertalanffy growth function (VBGF) fitted to integer age data, the VBGF fitted to fractional age data, the Somers model, and the Pauly model used to examine the growth of the central sub-population of northern anchovy (*Engraulis mordax*) that ranges from Northern California to Baja California, Mexico. The model parameters are mean asymptotic length (L_∞); growth coefficients (K and K'); the theoretical age at which length is zero (t_0), the inflection point, or the amount of time between time zero and the start of the convex portion of the first sinusoidal growth oscillation (t_s); the proportional decrease in growth at the depth of the growth oscillation (C); and *no growth time* (NGT), or the length of the period of no growth as a fraction of a year. For each model, the Akaike information criterion (AIC) and the difference in its AIC value from that of the best model (the one with the lowest AIC) (ΔAIC) are provided. No AIC or ΔAIC values are given for the VBGF fitted to integer age data as that data set is different from the data set of fractional ages used with the other models. All models were fitted to length-at-age data for fish collected during fishery-independent and fishery-dependent surveys from 2015 through 2021. SL=standard length.

| | Parameter estimates (95% confidence intervals) | | | | | | | | |
Model	L_∞ (mm SL)	K (year^{-1})	K' ((1–NGT)$^{-1}$)	t_0 (years)	t_s (year)	C	NGT (year)	AIC	ΔAIC
VBGF (integer)	130.6 (129.1–132.3)	0.52 (0.47–0.56)	–	−2.51 (−2.68–−2.35)	–	–	–	–	–
VBGF (fractional)	125.1 (124.2–125.9)	0.73 (0.69–0.77)	–	−1.53 (−1.63–−1.45)	–	–	–	96,428.3	172.10
Somers model	126.2 (125.4–127.1)	0.68 (0.64–0.71)	–	−1.74 (−1.79–−1.67)	0.12 (0.10–0.15)	0.90 (0.77–1.00)	–	96,256.2	0.00
Pauly model	126.4 (125.5–127.4)	–	0.67 (0.63–0.73)	−1.76 (−1.81–−1.61)	0.13 (0.11–0.15)	–	0.00 (0.00–0.08)	96,257.9	1.69

assessments. When time or costs do not allow all samples that were measured for length to be aged, age–length keys (ALKs) are used to draw inferences about the age composition of a stock and are used in stock assessments to estimate growth or mortality rates (Coggins et al., 2013) and to estimate abundance and catch at age (Kimura, 1977). When ages and growth characteristics are estimated with extrapolation-based methods (e.g., ALKs), more errors are generated for populations with extensive overlap of length distributions across ages and large variability in length at age (Miranda and Colvin, 2017). These errors could propagate throughout an assessment when an ALK is used to calculate weight at age, as has been done in the CSNA stock assessment (Kuriyama et al., 2022), which is ultimately used to calculate recruitment and biomass quantities relevant for management of this population.

Although the VBGF is the most typical model used to describe growth of CPS on the U.S. Pacific coast (Armstrong and Shelton, 1990; Crone et al., 2019; Kuriyama et al., 2020, 2022), no other work has examined seasonal modifications to the VBGF for northern anchovy. We found that the best fitting growth model for the CSNA was the Somers model, which allows growth to oscillate seasonally. Seasonal growth oscillations have been reported for small CPS around the world: the European anchovy (*E. encrasicolus*) (Bellido et al., 2000; Bilgin et al., 2013), Peruvian anchoveta (*E. ringens*) (Palomares et al., 1987; Cubillos and Arancibia, 1993; Cerna and Plaza, 2016), European pilchard (*Sardina pilchardus*) (Silva et al., 2008), and Araucanian herring (*Strangomera bentincki*) (Cubillos et al., 2002; Feltrim and Ernst, 2010). However, in many

of the studies that generated these reports, length-based methods were used to estimate growth parameters with seasonal growth models, possibly yielding less reliable estimations than those from the use of age-based methods (Liu et al., 2021).

We found that the VBGF overestimated L_∞ and underestimated K in comparison to estimation with the Somers model, and Liu et al. (2021) had the same observation when seasonal growth oscillations of small species were ignored. The misestimation of growth parameters when seasonality is ignored can propagate biases in stock assessments because underestimating K results in underestimation of natural mortality and possibly in characterization of a stock as less productive than it actually is (Scherrer et al., 2021). Additionally, when seasonality was included with the estimation of fractional ages, overlaps in length at age were reduced, and that reduction may result in more accurate ALKs and, therefore, reduce bias in stock assessments.

Validating that otolith growth has a relationship with somatic growth is imperative, as it permits the use of data from otolith studies (e.g., increment widths) to test for relationships between fish growth and climate indices or regional environmental conditions, and information about such relationships is important for projections of climate- and ecosystem-level change on marine communities (Muhling et al., 2018; Erisman et al., 2021; Tommasi et al., 2021). The linear relationship between otolith length and fish length indicates that otolith growth does reflect somatic growth to a degree for the CSNA; however, it is not uncommon for otolith and somatic growth

to be decoupled because somatic growth is tied to the environment and otolith growth is tied to metabolic rate (Buckmeier et al., 2017).

The differences in otolith growth among seasons observed in our study may also provide examples of the uncoupling of otolith and somatic growth reported for some other fish species that have seasonally different growth rates (e.g., Francis et al., 1993). In the summer season, when the fastest growth was found, mean otolith length for fish of a given length was smaller than that for fish in other seasons (and growth rates were lower), with seasonal differences diminished at larger fish lengths (greater than ~120 mm SL). The larger otolith lengths in winter may also indicate that otoliths continue to grow in seasons during which somatic growth is reduced, a common phenomenon (Secor and Dean, 1992; Buckmeier et al., 2017). The negative relationship between otolith size and somatic growth rate is predicted for individuals growing according to the VBGF (Xiao, 1996), but the presence of a strong growth effect can create substantial errors for studies in which otoliths are used to back-calculate fish length (Campana, 1990). Although we did not directly test the effect of growth rates on the relationship between otolith length and fish length, the results of our study provide a starting point for examination of this relationship in the future.

One potential source of uncertainty in this study is the sample distribution. Only 162 fish (0.008%) in our study were <50 mm SL, possibly a reflection of the selectivity of the commercial fishery, size selectivity of trawl nets, locality of trawl tows, or a combination of these factors. The commercial fishery is known to avoid small fish (generally <90 mm SL) because small individuals may clog nets (Huppert et al., 1980). More importantly, the fishery is extremely limited by market demand because large anchovies have a higher fat content and are, therefore, more desirable for their main uses as feed for the finfish mariculture industry, pet food, oil for pharmaceuticals, live bait, and fresh or canned food for human consumption (CDFW, 2022; Kuriyama et al., 2022). Therefore, fishery-dependent data will consistently have this source of uncertainty, and fishery-independent data can help fill this gap.

The net used in SWFSC acoustic-trawl surveys has an 8-mm mesh liner to retain juvenile and adult fish as small as 50 mm SL and potentially as large as 800 mm SL (Dotson and Griffith, 1996; Dotson et al., 2010; Dorval et al., 2022), but small fish are known to be poorly represented in catches made with nets with similar sizes of mesh liner in contrast to their representation in purse seine samples (Dotson and Griffith, 1996). Small juveniles of the CSNA tend to remain closer to shore (Parrish et al., 1985), but NOAA research vessels are unable to operate in waters with depths less than 20–30 m. Therefore, any CPS aggregations in shallow, nearshore areas are missed; it should be noted that the SWFSC is addressing this data gap through the inclusion of sampling of nearshore areas by commercial fishing vessels with the sampling conducted during its fishery-independent surveys (Dorval et al., 2022; Renfree et al., 2022). Except for 1 individual,

all fish <50 mm SL were caught in 2015, the year in which abundances of young of the year in the CSNA were found to have increased drastically (Zwolinski et al., 2017; Thompson et al., 2019). The presence of small individuals in 2015 indicates that small fish (<50 mm SL) will be collected when they are present in high numbers with the current sampling design and trawl net.

The disproportionate distribution of samples from both the fishery-independent and fishery-dependent surveys, with a decline in older age classes (>4 years), may also be due to the sampling designs used. The commercial fishery fleet fishes anchovy close to shore, where younger fish are common (Parrish et al., 1985), and close to ports because fish do not survive well in the holds over the time it takes to cover long distances from shore (Kuriyama et al., 2022). The SWFSC trawl survey is designed to sample the entire populations of CPS to assess their biomass (Stierhoff et al., 2020), a different objective than that of a survey focused purely on age and growth in which ideally all age classes are sampled uniformly regardless of relative abundance (Bolser et al., 2018).

It is important to ensure that growth data accurately represent the variability of the lengths at each age, as sampling that is not representative of the underlying population may produce biased estimates of growth characteristics and mortality (Sainsbury, 1980; Goodyear, 2019). Further sampling of older age classes could cause the current estimates of growth characteristics to change, but attempting to add samples in size bins for which catch is more rare in size-stratified sampling can substantially increase bias in mean size estimates (Goodyear, 2019). The current 2-stage sampling design of the SWFSC trawl survey meets both of these important needs through minimization of bias due to sampling distribution by first selecting samples at random so that they are representative of what is caught and then by making sure a sufficient number of otoliths from all length (and age) classes of a species or population are aged to accurately approximate the true variation in length at age (Schwartzkopf et al., 2022).

The high percentage of fish from age 0 to age 2 in sampling and the low percentage of fish at age 4+ reflect the current belief that the maximum age of northern anchovy has declined over time with catches being heavily dominated by age-0 and age-1 fish and having diminished levels of older age groups (Mais, 1981; MacCall, 2009). This result is in line with a high mortality rate typical of clupeoids (Armstrong and Shelton, 1990) and the CSNA (Kuriyama et al., 2022), assuming that the survey samples are representative of the adult population. Given the low harvest rate by the commercial fishery (PFMC, 2022), it is reasonable to conclude that the high mortality rates reflect natural mortality (e.g., mortality that results from predation or starvation). Additionally, true length at age may be underestimated because slower-growing marine fish can have higher predation mortality rates (Fennie et al., 2020). The northern subpopulation of northern anchovy is thought to have larger, older, and faster-growing fish than those in the CSNA (Parrish et al., 1985; Stierhoff et al., 2020; senior author, unpubl. data). Future work could

examine growth characteristics for the entire species with the addition of older individuals (>4 years old) as well as could compare characteristic estimates between subpopulations and stratify by latitude.

Conclusions

This work is the first comprehensive investigation into modeling non-seasonal and seasonal growth oscillations in northern anchovy by using an age-based method. The results indicate the importance of incorporating seasonality when modeling somatic growth of CPS with data from samples collected year-round. If seasonality is ignored, L_∞ may be overestimated and growth coefficients (i.e., K) may be underestimated. The similarity in parameter estimates from the VBGF fitted to integer age data when only 2 months of data were included and from the Somers model fitted to fractional age data when data from year-round sampling were included indicates that 1) the seasonal model appears to account well for seasonal growth oscillations of the CSNA and 2) a VBGF fitted with integer ages may be appropriate for use with data collected over a short time period. Accurately describing growth is important to decrease biases that may propagate in stock assessments and subsequently in management decisions.

Resumen

Los parámetros de crecimiento somático se utilizan en modelos de evaluación de poblaciones estructurados por edades, como los que se emplean para evaluar y manejar federalmente la anchoa del norte (*Engraulis mordax*); por lo tanto, un estimado incorrecto del crecimiento puede causar errores que afecten a los estimados de las evaluaciones de poblaciones. Hasta donde sabemos, hemos completado la primera investigación exhaustiva para modelar el crecimiento somático y de los otolitos de la subpoblación central de la anchoa del norte (CSNA), que tiene su distribución desde el norte de California hasta Baja California, México, utilizando datos dependientes e independientes de la pesca. Para determinar el modelo que mejor describía el crecimiento, se ajustaron cinco modelos de crecimiento a los datos de talla por edad, incluidos 2 modelos que tienen en cuenta las oscilaciones estacionales del crecimiento. Se observaron oscilaciones estacionales del crecimiento en el CSNA, y los modelos que mejor se ajustaban fueron los que tenían en cuenta la estación. El crecimiento más rápido se produjo durante el verano, y disminuyó 90% en invierno. Se observaron grandes variaciones en la longitud a la edad y un amplio solapamiento de longitudes entre edades en el CSNA, observaciones típicas de peces con un modo de vida oportunista que responden rápidamente a las condiciones ambientales cambiantes en ecosistemas dinámicos. Los modelos de crecimiento tradicionales sobrestimaron la longitud asintótica media y subestimaron el coeficiente de crecimiento en comparación con los resultados de los modelos de crecimiento estacional. Describir con precisión

el crecimiento de la CSNA teniendo en cuenta la estacionalidad es importante para limitar los sesgos que pueden propagarse en las evaluaciones de las poblaciones y en las decisiones de manejo.

Acknowledgments

Literature cited

Adams, P. B.
  1980. Life history patterns in marine fishes and their consequences for fisheries management. Fish. Bull. 78:1–12.
Akaike, H.
  1973. Information theory as an extension of the maximum likelihood principle. *In* Second International Symposium on Information Theory; Tsahkadsor, 2–8 September 1971 (B. N. Petrov and F. Csáki, eds.), p. 267–281. Akadémiai Kiadó, Budapest, Hungary.
Aldanondo, N., U. Cotano, P. Alvarez, and A. Uriarte.
  2016. Validation of the first annual increment deposition in the otoliths of European anchovy in the Bay of Biscay based on otolith microstructure analysis. Mar. Freshw. Res. 67:943–950. Crossref
Armstrong, M. J., and P. A. Shelton.
  1990. Clupeoid life-history styles in variable environments. Environ. Biol. Fishes 28:77–85. Crossref
Bacha, M., A. Moali, N.-E. Benmansour, J.-M. Brylinski, K. Mahé, and R. Amara.
  2010. Relationships between age, growth, diet and environmental parameters for anchovy (*Engraulis encrasicolus* L.) in the Bay of Bénisaf (SW Mediterranean, west Algerian coast). Cybium 34:47–57. Crossref
Barbosa, A. M., R. Real, A.-R. Muñoz, and J. A. Brown.
  2013. New measures for assessing model equilibrium and prediction mismatch in species distribution models. Divers. Distrib. 19:1333–1338. Crossref
Basilone, G., M. Barra, R. Ferreri, S. Mangano, M. Pulizzi, G. Giacalone, I. Fontana, S. Aronica, A. Gargano, P. Rumolo, et al.
  2020. First annulus formation in the European anchovy; a two-stage approach for robust validation. Sci. Rep. 10:1079. Crossref
Baty, F., C. Ritz, S. Charles, M. Brutsche, J.-P. Flandrois, and M.-L. Delignette-Muller.
  2015. A toolbox for nonlinear regression in R: the package nlstools. J. Stat. Softw. 66(5):1–21. Crossref
Bellido, J. M., G. J. Pierce, J. L. Romero, and M. Millán.
  2000. Use of frequency analysis methods to estimate growth of anchovy (*Engraulis encrasicolus* L. 1758) in the Gulf of Cádiz (SW Spain). Fish. Res. 48:107–115. Crossref
Beverton, R. J. H., and S. J. Holt.
  1957. On the dynamics of exploited fish populations. Minist. Agric. Fish. Food, Fish Invest. ser. 2, vol. 19, 533 p. HMSO, London.

Bilgin, S., B. Taşçi, and H. Bal.
  2013. Sexual seasonal growth of the European anchovy (*Engraulis encrasicolus*) caught by mid-water trawl and purse seine in the southern Black Sea. J. Mar. Biol. Assoc. UK. 93:333–339. Crossref
Blaxter, J. H. S., and J. R. Hunter.
  1982. The biology of the clupeoid fishes. Adv. Mar. Biol. 20:3–223. Crossref
Bolser, D. G., A. Grüss, M. A. Lopez, E. M. Reed, I. Mascareñas-Osorio, and B. E. Erisman.
  2018. The influence of sample distribution on growth model output for a highly-exploited [sic] marine fish, the Gulf Corvina (*Cynoscion othonopterus*). PeerJ 6:e5582 Crossref
Brosset, P., J. Lloret, M. Muñoz, C. Fauvel, E. Van Beveren, V. Marques, J.-M. Fromentin, F. Ménard, and C. Saraux.
  2016. Body reserves mediate trade-offs between life-history traits: new insights from small pelagic fish reproduction. R. Soc. Open Sci. 3:160202. Crossref
Buckmeier, D. L., P. C. Sakaris, and D. J. Schill.
  2017. Validation of annual and daily increments in calcified structures and verification of age estimates. *In* Age and growth of fishes: principles and techniques (M. C. Quist and D. A. Isermann, eds.), p. 33–79. Am. Fish. Soc., Bethesda, MD.
Burnham, K. P., and D. R. Anderson.
  2002. Model selection and multi-modal inference: a practical information-theoretical approach, 488 p. Springer, New York.
Burnham, K. P., D. R. Anderson, and K. P. Huyvaert.
  2011. AIC model selection and multimodal inference in behavior ecology: some background, observations, and comparisons. Behav. Ecol. Sociobiol. 65:23–35. Crossref
Butler, J. L.
  1989. Growth during the larval and juvenile stages of the northern anchovy, *Engraulis mordax*, in the California Current during 1980–84. Fish. Bull. 87:645–652.
Campana, S. E.
  1990. How reliable are growth back-calculations based on otoliths? Can. J. Fish. Aquat. Sci. 47:2219–2227. Crossref
Campana, S. E., and C. M. Jones.
  1992. Analysis of otolith microstructure data. *In* Otolith microstructure examination and analysis (D. K. Stevenson, and S. E. Campana, eds.), p. 73–100. Can. Spec. Publ. Fish. Aquat. Sci. 117.
CDFW (California Department of Fish and Wildlife).
  2022. Northern anchovy. Last modified 6 April 2022. website
Cerna, F., and G. Plaza.
  2016. Daily growth patterns of juveniles and adults of the Peruvian anchovy (*Engraulis ringens*) in northern Chile. Mar. Freshw. Res. 67:899–912. Crossref
Checkley, D. M., Jr., and J. A. Barth.
  2009. Patterns and processes in the California Current System. Prog. Oceanogr. 83:49–64. Crossref
Cisneros, M. A., J. Estrada, and G. Montemayer.
  1990. Growth, mortality and recruitment of exploited small pelagic fishes in the Gulf of California, Mexico. Fishbyte 8:15–17.
Claireaux, M., T. C. dos Santos Schmidt, E. M. Olsen, A. Slotte, Ø. Varpe, M. Heino, and K. Enberg.
  2021. Eight decades of adaptive changes in herring reproductive investment: the joint effect of environment and exploitation. ICES J. Mar. Sci. 78:631–639. Crossref
Coggins, L. G., Jr., D. C. Gwinn, and M. S. Allen.
  2013. Evaluation of age–length key sample sizes required to estimate fish total mortality and growth. Trans. Am. Fish. Soc. 142:832–840. Crossref

Collins, R. A.
  1969. Size and age composition of northern anchovies (*Engraulis mordax*) in the California anchovy reduction fishery for the 1965–66, 1966–67, and 1967–68 seasons. *In* The northern anchovy (*Engraulis mordax*) and its fishery 1965–1968, p. 56–74. Calif. Dep. Fish Game, Fish Bull. 147.
Collins, R. A., and J. D. Spratt.
  1969. Age determination of northern anchovies, *Engraulis mordax*, from otoliths. *In* The northern anchovy (*Engraulis mordax*) and its fishery 1965–1968, p. 39–55. Calif. Dep. Fish Game, Fish Bull. 147.
Crone, P. R., K. T. Hill, J. P. Zwolinski, and M. J. Kinney.
  2019. Pacific mackerel (*Scomber japonicus*) stock assessment for U.S. management in the 2019–20 and 2020–21 fishing years, 112 p. Pac. Fish. Manage. Counc., Portland, OR. [Available from website.]
Cubillos, L., and H. Arancibia.
  1993. On the seasonal growth of common sardine (*Strangomera bentincki*) and anchovy (*Engraulis ringens*) off Talcahuanon, Chile. Rev. Biol. Mar. (Valparaíso) 28:43–49.
Cubillos, L. A., D. F. Arcos, D. A. Bucarey, and M. T. Canales.
  2001. Seasonal growth of small pelagic fish off Talcahuano, Chile (37°S, 73°W): a consequence of their reproductive strategy to seasonal upwelling? Aquat. Living Resour. 14:115–124. Crossref
Cubillos, L. A., D. A. Bucarey, and M. Canales.
  2002. Monthly abundance estimation for common sardine *Strangomera bentincki* and anchovy *Engraulis ringens* in the central-southern area off Chile (34–40°S). Fish. Res. 57:117–130. Crossref
Dorval, E., B. J. Macewicz, D. A. Griffith, and Y. Gu.
  2018. Spawning biomass of the central stock of northern anchovy (*Engraulis mordax*) estimated from the daily egg production method off California in 2017. NOAA Tech. Memo. NMFS-SWFSC-607, 31 p.
Dorval, E., D. Porzio, B. D. Schwartzkopf, K. C. James, L. Vasquez, and B. Erisman.
  2022. Sampling methodology for estimating life history parameters of coastal pelagic species along the U.S. Pacific coast. NOAA Tech. Memo. NMFS-SWFSC-660, 40 p.
Dotson, R. C., and D. A. Griffith.
  1996. A high-speed midwater rope trawl for collecting coastal pelagic fishes. CalCOFI Rep. 37:134–139. [Available from website.]
Dotson, R. C., D. A. Griffith, D. L. King, and R. L. Emmett.
  2010. Evaluation of a marine mammal excluder device (MMED) for a Nordic 264 midwater rope trawl. NOAA Tech. Memo. NMFS-SWFSC-455, 14 p.
Erisman, B. E., E. M. Reed, M. J. Román, I. Mascareñas-Osorio, P. van der Sleen, C. López-Sagástegui, O. Aburto-Oropeza, K. Rowell, and B. A. Black.
  2021. Relationships among somatic growth, climate, and fisheries production in an overexploited marine fish from the Gulf of California, Mexico. Fish. Oceanogr. 30:556–568. Crossref
Feltrim, M., and B. Ernst.
  2010. Inter-cohort growth variability and its implication for fishery management of the common sardine (*Strangomera bentincki*) stock off the coast of south-central Chile. Fish. Res. 106:368–377. Crossref
Fennie, H. W., S. Sponaugle, E. A. Daly, and R. D. Brodeur.
  2020. Prey tell: what quillback rockfish early life history traits reveal about their survival in encounters with juvenile coho salmon. Mar. Ecol. Prog. Ser. 650:7–18. Crossref
Fournier, D., and C. P. Archibald.
  1982. A general theory for analyzing catch at age data. Can. J. Fish. Aquat. Sci. 39:1195–1207. Crossref

Francis, M. P., M. W. Williams, A. C. Pryce, S. Pollard, and S. G. Scott.
1993. Uncoupling of otolith and somatic growth in *Pagrus auratus* (Sparidae). Fish. Bull. 91:159–164.

García-Berthou, E., G. Carmona-Catot, R. Merciai, and D. H. Ogle.
2012. A technical note on seasonal growth models. Rev. Fish Biol. Fish. 22:635–640. Crossref

Gompertz, B.
1825. On the nature of the function expressive of the law of human mortality, and on a new mode of determining the value of life contingencies. In a letter to Francis Baily, Esq. F. R. S. &c. Philos. Trans. R. Soc. Lond. 115:513–583. Crossref

Goodyear, C. P.
2019. Modeling growth: consequences from selecting samples by size. Trans. Am. Fish. Soc. 148:528–551. Crossref

Guisan, A., and N. E. Zimmermann.
2000. Predictive habitat distribution models in ecology. Ecol. Model. 135:147–186. Crossref

Hoenig, N., and R. Choudaray Hanumara.
1982. A statistical study of a seasonal growth model for fishes. Univ. Rhode Island, Dep. Comput. Sci. Stat., Tech. Rep., 91 p.

Hunter, J. R., and R. Leong.
1981. The spawning energetics of female northern anchovy, *Engraulis mordax*. Fish. Bull. 79:215–230.

Hunter, J. R., and B. J. Macewicz.
1980. Sexual maturity, batch fecundity, spawning frequency, and temporal pattern of spawning for the northern anchovy, *Engraulis mordax*, during the 1979 spawning season. CalCOFI Rep. 21:139–149. [Available from website.]
1985. Rates of atresia in the ovary of captive and wild northern anchovy, *Engraulis mordax*. Fish. Bull. 83:119–136.

Huppert, D. D., A. D. MacCall, G. D. Stauffer, K. R. Parker, J. A. McMillan, and H. W. Frey.
1980. California's northern anchovy fishery: biological and economic basis for fishery management. NOAA Tech. Memo. NMFS-SWFSC-1, 121 p.

Jacox, M. G., C. A. Edwards, E. L. Hazen, and S. J. Bograd.
2018. Coastal upwelling revisted: Ekman, Bakun, and improved upwelling indices for the U.S. West Coast. J. Geophys. Res. Oceans 123:7332–7350. Crossref

Kerns, J. A., and L. A. Lombardi-Carlson.
2017. History and importance of age and growth information. In Age and growth of fishes: principles and techniques (M. C. Quist and D. A. Isermann, eds.), p. 1–8. Am. Fish. Soc., Bethesda, MD.

Kimura, D. K.
1977. Statistical assessment of the age–length key. J. Fish. Res. Board Can. 34:317–324. Crossref

King, J. R., and G. A. McFarlane.
2003. Marine fish life history strategies: applications to fishery management. Fish. Manag. Ecol. 10:249–264. Crossref

Koehn, L. E., T. E. Essington, K. N. Marshall, W. J. Sydeman, A. I. Szoboszlai, and J. A. Thayer.
2017. Trade-offs between forage fish fisheries and their predators in the California Current. ICES J. Mar. Sci. 74:2448–2458. Crossref

Kozlowski, J.
1996. Optimal allocation of resources explains interspecific life-history patterns in animals with indeterminate growth. Proc. R. Soc., B 263:559–566. Crossref

Kuriyama, P. T., J. P. Zwolinski, K. T. Hill, and P. R. Crone.
2020. Assessment of the Pacific sardine resource in 2020 for U.S. management in 2020–2021. NOAA Tech. Memo. NMFS-SWFSC-628, 117 p.

Kuriyama, P. T., J. P. Zwolinski, S. L. H. Teo, and K. T. Hill.
2022. Assessment of the northern anchovy (*Engrualis mordax*) central subpopulation in 2021 for U.S. management. NOAA Tech. Memo. NMFS-SWFSC-665, 91 p.

Lasker, R.
1981. Factors contributing to variable recruitment of the northern anchovy *Engraulis mordax* in the California Current USA contrasting years 1975–1978. Rapp. P.-v. Réun. Cons. Int. Explor. Mer 178:375–388.

Lasker, R., and J. R. Zweifel.
1978. Growth and survival of first-feeding northern anchovy larvae (*Engraulis mordax*) in patches containing different proportions of large and small prey. In Spatial pattern in plankton communities, NATO Conf. Ser., vol. 3 (J. H. Steele, ed.), p. 329–354. Springer Science+Business Media, New York.

Lecomte, F., W. S. Grant, J. J. Dodson, R. Rodríguez-Sánchez, and B. W. Bowen.
2004. Living with uncertainty: genetic imprints of climate shifts in East Pacific anchovy (*Engraulis mordax*) and sardine (*Sardinops sagax*). Mol. Ecol. 13:2169–2182. Crossref

Libungan, L. A., and S. Pálsson.
2015. ShapeR: an R package to study otolith shape variation among fish populations. PLoS ONE 10(3):e0121102. Crossref

Litz, M. N. C., R. D. Brodeur, R. L. Emmett, S. S. Heppell, R. S. Rasmussen, L. O'Higgins, and M. S. Morris.
2010. Effects of variable oceanographic conditions on forage fish lipid content and fatty acid composition in the northern California Current. Mar. Ecol. Prog. Ser. 405:71–85. Crossref

Liu, Y., C. Zhang, C. Xu, Y. Xue, Y. Ren, and Y. Chen.
2021. Accounting for seasonal growth in per-recruit analyses: a case study of four commercial fish in coastal China Seas. Front. Mar. Sci. 8:567240. Crossref

Lo, N. C. H., P. E. Smith, and J. L. Butler.
1995. Population growth of northern anchovy and Pacific sardine using stage-specific matrix models. Mar. Ecol. Prog. Ser. 127:15–26. Crossref

MacCall, A. D.
2009. Mechanisms of low-frequency fluctuations in sardine and anchovy populations. In Climate change and small pelagic fish (D. Checkley, J. Alheit, Y. Oozeki, and C. Roy, eds.), p. 285–299. Cambridge Univ. Press, Cambridge, UK.

MacCall, A. D., W. J. Sydeman, P. C. Davison, and J. A. Thayer.
2016. Recent collapse of northern anchovy biomass off California. Fish. Res. 175:87–94. Crossref

Mais, K. F.
1981. Age-composition changes in the anchovy, *Engraulis mordax*, central population. CalCOFI Rep. 22:82–87. [Available from website.]

Mallicoate, D. L., and R. H. Parrish.
1981. Seasonal growth patterns of California stocks of northern anchovy, *Engraulis mordax*, Pacific mackerel, *Scomber japonicus*, and jack mackerel, *Trachurus symmetricus*. CalCOFI Rep. 22:69–81. [Available from website.]

McClatchie, S.
2014. Regional fisheries oceanography of the California Current system: the CalCOFI program, 235 p. Springer Science+Business Media, Dordrecht, Netherlands.

McHugh, J. L.
1951. Meristic variations and populations of northern anchovy (*Engraulis mordax mordax*). Bull. Scripps Inst. Oceanogr. Univ. Calif. 6:123–160.

Methot, R. D., Jr.
1983. Seasonal variation in survival of larval northern anchovy, *Engraulis mordax*, estimated from the age distribution of juveniles. Fish. Bull. 81:741–750.

1989. Synthetic estimates of historical abundance and mortality for northern anchovy. Am. Fish. Soc. Symp. 6:66–82.

Miranda, L. E., and M. E. Colvin.
2017. Sampling for age and growth estimation. *In* Age and growth of fishes: principles and techniques (M. C. Quist and D. A. Isermann, eds.), p. 107–125. Am. Fish. Soc., Bethesda, MD.

Muhling, B., M. Lindegren, L. W. Clausen, A. Hobday, and P. Lehodey.
2018. Impacts of climate change on pelagic fish and fisheries. *In* Climate change impacts on fisheries and aquaculture: a global analysis (B. F. Phillips and M. Pérez-Ramírez, eds.), p. 771–814. John Wiley & Sons, New York.

Muhling, B., S. Brodie, O. Snodgrass, D. Tommasi, H. Dewar, D. Tommas, J. Childers, M. Jacox, C. A. Edwards, Y. Xu, et al.
2019. Dynamic habitat use of albacore and their primary prey species in the California Current System. CalCOFI Rep. 60:79–93. [Available from website.]

Muhling, B. A., S. Brodie, J. A. Smith, D. Tommasi, C. F. Gaitan, E. L. Hazen, M. G. Jacox, T. D. Auth, and R. D. Brodeur.
2020. Predictability of species distributions deteriorates under novel environmental conditions in the California Current System. Front. Mar. Sci. 7:589. Crossref

Ogle, D. H.
2017. An algorithm for the von Bertalanffy seasonal cessation in growth function of Pauly et al. (1992). Fish. Res. 185:1–5. Crossref

Ogle, D. H., T. O. Brenden, and J. K. McCormick.
2017. Growth estimation: growth models and statistical inference. *In* Age and growth of fishes: principles and techniques (M. C. Quist and D. A. Isermann, eds.), p. 265–359. Am. Fish. Soc., Bethesda, MD.

Ogle, D. H., J. C. Doll, P. Wheele r, and A. Dinno.
2022. FSA: simple fisheries stock assessment methods. R package, vers. 0.9.3. [Available from website.]

Palance, D. G., B. J. Macewicz, K. Stierhoff, D. A. Demer, and J. P. Zwolinski.
2019. Length conversions and mass–length relationships of five forage-fish species in the California Current ecosystem. J. Fish Biol. 95:1116–1124. Crossref

Palomares, M. L., P. Muck, J. Mendo, E. Chuman, O. Gomez, and D. Pauly.
1987. Growth of the Peruvian anchoveta (*Engraulis ringens*), 1953 to 1982. *In* The Peruvian anchoveta and its upwelling ecosystem: three decades of change (D. Pauly and I. Tsukayama, eds.), p. 117–141. ICLARM Stud. Rev.15. Inst. Mar Peru (IMARPE), Callao, Peru; Dtsch. Ges. Tech. Zusammenarbeit (GTZ), Eschborn, Germany; Int. Cent. Living Aquat. Resour. Manage. (ICLARM), Manila, Philippines.

Parrish, R. H., D. L. Mallicoate, and K. F. Mais.
1985. Regional variations in the growth and age composition of northern anchovy, *Engraulis mordax*. Fish. Bull. 83:483–496.

Parrish, R. H., D. L. Mallicoate, and R. A. Klingbeil.
1986. Age dependent fecundity, number of spawnings per year, sex ratio, and maturation stages in northern anchovy, *Engraulis mordax*. Fish. Bull. 84:503–517.

Pauly, D., M. Soriano-Bartz, J. Moreau, and A. Jarre-Teichmann.
1992. A new model accounting for seasonal cessation of growth in fishes. Aust. J. Mar. Freshw. Res. 43:1151–1156. Crossref

PFMC (Pacific Fishery Management Council).
2019. Coastal pelagic species fishery management plan as amended through Amendment 17, 49 p. Pac. Fish. Manage. Counc., Portland, OR. [Available from website.]
2022. Status of the Pacific coast coastal pelagic species fishery and recommended acceptable biological catches.

Stock assessment and fishery evaluation 2021, including information through June 2021, 95 p. Pac. Fish. Manage. Counc., Portland, OR. [Available from website.]

R Core Team.
2022. R: a language and environment for statistical computing. R Foundation for Statistical Computing, Vienna, Austria. [Availbale from website, accessed July 2022.]

Reeves, S. A.
2003. A simulation study of the implications of age-reading errors for stock assessment and management advice. ICES J. Mar. Sci. 60:314–328. Crossref

Reiss, C. S., D. M. Checkley Jr., and S. J. Bograd.
2008. Remotely sensed spawning habitat of Pacific sardine (*Sardinops sagax*) and Northern [sic] anchovy (*Engraulis mordax*) within the California Current. Fish. Oceanogr. 17:126–136. Crossref

Renfree, J. S., N. M. Bowlin, B. E. Erisman, R. I. Rojas-González, G. E. Johnson, S. A. Mau, D. W. Murfin, B. D. Schwartzkopf, T. S. Sessions, K. L. Stierhoff, et al.
2022. Report on the summer 2021 California Current Ecosystem Survey (CCES) (2107RL), 6 July to 15 October 2021, conducted aboard NOAA ship [sic] *Reuben Lasker*, Mexican research vessel *Dr. Jorge Crranza Fraser*, fishing vessels *Lisa Marie* and *Long Beach Carnage*, and uncrewed surface vehicles. NOAA Tech. Memo. NMFS-SWFSC-669, 34 p.

Richards, L. J., J. T. Schnute, A. R. Kronlund, and R. J. Beamish.
1992. Statistical models for the analysis of ageing error. Can. J. Fish. Aquat. Sci. 49:1801–1815. Crossref

Ricker, W. E.
1975. Computation and interpretation of biological statistics of fish populations. Bull. Fish. Res. Board Can. 191:1–382.

Sainsbury, K. J.
1980. Effect of individual variability on the von Bertalanffy growth equation. Can. J. Fish. Aquat. Sci. 37:241–247. Crossref

Scherrer, S. R., D. R. Kobayashi, K. C. Weng, H. Y. Okamoto, F. G. Oishi, and E. C. Franklin.
2021. Estimation of growth parameters integrating tag-recapture, length-frequency, and direct aging data using likelihood and Bayesian methods for the tropical deepwater snapper *Pristipomoide filamentosus* in Hawaii. Fish. Res. 233:105753. Crossref

Schwartzkopf, B. D., E. Dorval, K. C. James, J. M. Walker, O. E. Snodgrass, D. L. Porzio, and B. E. Erisman.
2022. A summary report on life history information on the central subpopulation of Northern Anchovy (*Engraulis mordax*) for the 2021 stock assessment. NOAA Tech. Memo. NMFS-SWFSC-659, 67 p.

Secor, D. H., and J. M. Dean.
1992. Comparison of otolith-based back-calculation methods to determine individual growth histories of larval striped bass, *Morone saxatilis*. Can. J. Fish. Aquat. Sci. 49:1439–1454. Crossref

Shoup, D. E., and P. H. Michaletz.
2017. Growth estimation: summarization. *In* Age and growth of fishes: principles and techniques (M. C. Quist and D. A. Isermann, eds.), p. 233–264. Am. Fish. Soc., Bethesda, MD.

Silva, A., P. Carrera, J. Masse, A. Uriarte, M. B. Santos, P. B. Oliveira, E. Soares, C. Porteiro, and Y. Stratoudakis.
2008. Geographic variability of sardine growth across the northeastern Atlantic and the Mediterranean Sea. Fish. Res. 90:56–69. Crossref

Somers, I. F.
1988. On a seasonally oscillating growth function. Fishbyte 6:8–11.

Spratt, J. D.
　1975. Growth rate of the northern anchovy, *Engraulis mordax*, in southern California waters, calculated from otoliths. Calif. Fish Game 61:116–126.

Stawitz, C. C., M. A. Haltuch, and K. F. Johnson.
　2019. How does growth misspecification affect management advice derived from an integrated fisheries stock assessment model? Fish. Res. 213:12–21. Crossref

Stierhoff, K. L., J. P. Zwolinski, and D. A. Demer.
　2019. Distribution, biomass, and demography of coastal pelagic fishes in the California Current Ecosystem during summer 2018 based on acoustic-trawl sampling. NOAA Tech. Memo. NMFS-SWFSC-613, 63 p.
　2020. Distribution, biomass, and demography of coastal pelagic fishes in the California Current Ecosystem during summer 2019 based on acoustic-trawl sampling. NOAA Tech. Memo. NMFS-SWFSC-626, 80 p.
　2021a. Distribution, biomass, and demography of coastal pelagic fishes in the California Current Ecosystem during summer 2016 based on acoustic-trawl sampling. NOAA Tech. Memo. NMFS-SWFSC-649, 79 p.
　2021b. Distribution, biomass, and demography of coastal pelagic fishes in the California Current Ecosystem during summer 2015 based on acoustic-trawl sampling. NOAA Tech. Memo. NMFS-SWFSC-648, 57 p.

Sydeman, W. J., S. Dedman, M. García-Reyes, S. A. Thompson, J. A. Thayer, A. Bakun, and A. D. MacCall.
　2020. Sixty-five years of northern anchovy population studies in the southern California Current: a review and suggestion for sensible management. ICES J. Mar. Sci. 77:486–499. Crossref

Takahashi, M., D. M. Checkley Jr., M. N. C. Litz, R. D. Brodeur, and W. T. Peterson.
　2012. Responses in growth rate of larval northern anchovy (*Engraulis mordax*) to anomalous upwelling in the northern California Current. Fish. Oceanogr. 21:393–404. Crossref

Thayer, J. A., A. D. MacCall,, W. J. Sydeman, and P. C. Davison.
　2017. California anchovy population remains low, 2012–2016. CalCOFI Rep. 58:69–76. [Available from website.]

Thomas, R. M.
　1983. Seasonal variation in the relationship between otolith radius and fish length in the pilchard off South West Africa. S. Afr. J. Mar. Sci. 1:133–138. Crossref

Thompson, A. R., I. D. Schroeder, S. J. Bograd, E. L. Hazen, M. G. Jacox, A. Leising, B. K. Wells, J. L. Largier, J. L. Fisher, K. C. Jacobson, et al.
　2019. State of the California Current 2018–19: a novel anchovy regime and a new marine heat wave? CalCOFI Rep. 60:1–65. [Available from website.]

Thompson, A. R., E. P. Bjorkstedt, S. J. Bograd, J. L. Fisher, E. L. Hazen, A. Leising, J. A. Santora, E. V. Satterthwaite, W. J. Sydeman, M. Alksne, et al.
　2022. State of the California Current Ecosystem in 2021: winter is coming? Front. Mar. Sci. 9:958727. Crossref

Tommasi, D., Y. deReynier, H. Townsend, C. J. Harvey, W. H. Satterthwaite, K. N. Marshall, I. C. Kaplan, S. Brodie, J. C. Field, E. L. Hazen, et al.
　2021. A case study in connecting fisheries management challenges with models and analysis to support ecosystem-based management in the California Current Ecosystem. Front. Mar. Sci. 8:624161. Crossref

Uriarte, A., I. Rico, B. Villamor, E. Duhamel, C. Dueñas, N. Aldanondo, and U. Cotano.
　2016. Validation of age determination using otoliths of the European anchovy (*Engraulis encrasicolus* L.) in the Bay of Biscay. Mar. Freshw. Res. 67:951–966. Crossref

von Bertalanffy, L.
　1938. A quantitative theory of organic growth (inquiries on growth laws. II). Hum. Biol. 10:181–213.

Vrooman, A. M., P. A. Paloma, and J. R. Zweifel.
　1981. Electrophoretic, morphometric, and meristic studies of subpopulations of northern anchovy, *Engraulis mordax*. Calif. Fish Game 67:39–51.

Winemiller, K. O., and K. A. Rose.
　1992. Patterns of life-history diversification in North American fishes: implications for population regulation. Can. J. Fish. Aquat. Sci. 49:2196–2218. Crossref

Xiao, Y.
　1996. How does somatic growth rate affect otolith size in fishes? Can. J. Fish. Aquat. Sci. 53:1675–1682. Crossref

Yaremko, M. L.
　1996. Age determination in Pacific sardine, *Sardinops sagax*. NOAA Tech. Memo. NMFS-SWFSC-223, 34 p.

Zwolinski, J. P., D. A. Demer, B. J. Macewicz, S. Mau, D. Murfin, D. Palance, J. S. Renfree, T. S. Sessions, and K. Stierhoff.
　2017. Distribution, biomass and demography of the central-stock of northern anchovy during summer 2016, estimated from acoustic-trawl sampling. NOAA Tech. Memo. NMFS-SWFSC-572, 18 p.

Zwolinski, J. P., K. L. Stierhoff, and D. A. Demer.
　2019. Distribution, biomass, and demography of coastal pelagic fishes in the California Current Ecosystem during summer 2017 based on acoustic-trawl sampling. NOAA Tech. Memo. NMFS-SWFSC-610, 56 p.